IEEE Access
Multidisciplinary | Rapid Review | Open Access Journal

Received September 6, 2019, accepted October 3, 2019, date of publication December 13, 2019, date of current version January 6, 2020.

Digital Object Identifier 10.1109/ACCESS.2019.2958965

Cause, Classification of Voltage Sag, and Voltage Sag Emulators and Applications: A Comprehensive Overview

YANG HAN[1], (Senior Member, IEEE), YU FENG[1], PING YANG[1], LIN XU[2], YAN XU[3], (Senior Member, IEEE), AND FREDE BLAABJERG[4], (Fellow, IEEE)

[1]School of Mechanical and Electrical Engineering, University of Electronic Science and Technology of China, Chengdu 611731, China
[2]Sichuan Electric Power Research Institute, Sichuan Electric Power Company, Chengdu 610041, China
[3]School of Electrical and Electronic Engineering, Nanyang Technological University, Singapore 639798
[4]Department of Energy Technology, Aalborg University, 9220 Aalborg, Denmark

Corresponding author: Yang Han (hanyang@uestc.edu.cn)

This work was supported in part by the Natural Science Foundation of Guangdong Province under Grant 2018A030313494, and in part by the State Key Laboratory of Alternate Electrical Power System with Renewable Energy Sources under Grant LAPS18007.

ABSTRACT The large-scale application of wind power and photovoltaic power solves the energy crisis and alleviates the environmental problems caused by the use of conventional energy. However, they are at risk of being randomly tripped from the network when faced to voltage sag and severe fault events, which will lead to a sudden reduction of active power output and also complicates fault recovery process of the whole system. Moreover, it may also aggravate failures and lead to large-scale power outages, which stimulates a growing interest in analyzing the low-voltage ride-through (LVRT) capabilities of the renewable energy systems (RES) and improving the performance through developing various mathematical models and analysis tools. In this paper, a systematical overview of cause, classification of voltage sag phenomena and voltage sag emulating techniques is presented, and four voltage sag generators (VSGs) are discussed and compared, which include generator based-VSG, shunt impedance based-VSG, transformer based-VSG and full converter based-VSG. Furthermore, a closed-loop detection platform based on real-time digital simulator (RTDS) for the converter controller of a permanent magnet synchronous generator (PWSG) set is introduced, to investigate the LVRT performance of the WT system under grid voltage sag conditions. Finally, the application of VSG in RES are presented and the future research directions are also discussed.

INDEX TERMS Voltage sag generator, renewable energy systems, low voltage ride through, power quality, distributed generation (DG), PV, wind power generation system.

I. INTRODUCTION

With the globally increasing electricity demand and a desire to bring down CO_2 emissions, a transition from fossil fuels to sustainable energy is needed [1]. In the past decades, the distributed generations (DGs), which are dominated by the wind power, photovoltaic (PV) power generation, fuel cell and gas/steam power plants, are gradually integrated into the distributed power system layers [2]–[4]. The distributed RESs, which are more scalable than central power plants, can be used locally or flexibly connected to the power systems [5], are gradually replacing the conventional power generation plants and playing an important part in the future smart grids [6], [7]. However, modern power systems and customers are becoming more and more sensitive to the quality of supplied power. On one hand, the electric devices in modern industry include a variety of the power electronic components, smart sensors and actuators, which can be very vulnerable to power system disturbances, such as voltage sag and swell, voltage variations, frequency deviations, harmonics, unbalance and other transient interruptions. On the other hand, the electrical customers become more susceptible to the power losses due to the equipment failure or malfunction. Among all types of power quality problems, the voltage sag is the most common events happened in power systems and it is the main problem in industry.

Generally, voltage sag is a temporary voltage magnitude reduction, which refers to the phenomenon of grid voltage

The associate editor coordinating the review of this manuscript and approving it for publication was Chandan Kumar.

amplitude variation when the duration is from one-half cycle to 1 min and the effective value of voltage drops rapidly to the rated value of 0.1 *p.u.* to 0.9 *p.u.* [8]–[11].

As illustrated in Fig. 1, natural disasters or load transient conditions may result in grid voltage sags, such as: climate conditions, the equipment failure of utility companies, bird nesting across the distribution lines, various short circuit failures, start-up of large electric motor, and lightning stroke, leading to shut-down or burnout of equipment, which brings detrimental effects to industrial manufacturing process and huge economic loss to the sensitive customers.

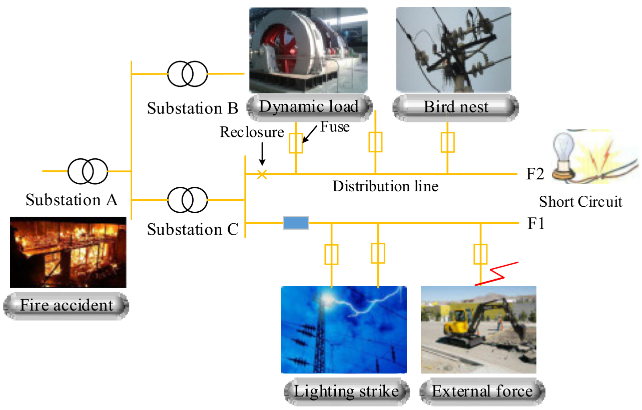

FIGURE 1. Overview of the cause of grid voltage sag event.

When voltage sag occurs due to remote fault conditions in the transmission or distribution networks, the sensitive load often trips or stops. Investigations show that more than 90% of power system disturbances are caused by voltage sags [12], [13]. In order to understand the effects of voltage sags on the sensitive and critical loads, as well as in renewable energy systems (RES), it is important to test the immunity of sensitive equipment under various voltage sag disturbances. Therefore, controllable voltage sag generators would be required with the variable voltages magnitudes, durations, and frequencies.

To understand the behavior of the sensitive load under grid sag conditions, and investigate the voltage sag immunity of the grid-connected power electronic converters, it is necessary to briefly review the fault ride-through regulation standards, as discussed in various grid codes and recent publications.

Fig. 2 shows a comparison of fault ride through capability requirements for wind turbines in China, Germany, Spain, US, and Denmark. The wind power grid-connection standards in China require wind turbines installed in wind farms to meet the dynamic adjustment of power factor in the range of 0.95 (leading) to 0.95 (lagging). However, the standards of other countries, such as Spain and Germany, require a more relaxed profile in the low voltage ride-through curve. Moreover, Germany, Britain and Canada all put forward a wider range of power factor of wind turbines. Germany requires that wind turbines have the ability to change at a constant speed

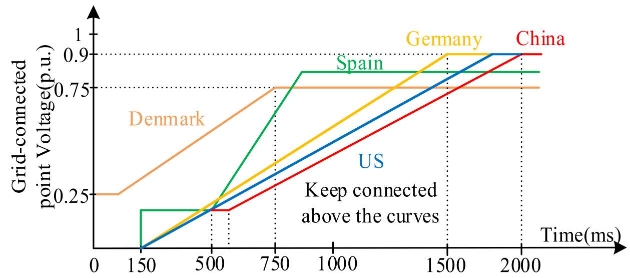

FIGURE 2. Comparison of fault ride-through capability requirement for wind turbines in Denmark, Span, Germany, US and China [14]–[15].

of 1% rated power per minute in the whole range between the minimum and the nominal power under continuous operation conditions. Moreover, under any operating conditions, wind turbines must be able to reduce active power output and climb from any operating point to the prescribed maximum power set point [14], [15].

For technical requirements of grid connected photovoltaic power plants, the Chinese standards are slightly different from the other standards in LVRT profile, which is discussed in [16], as shown in Fig. 3. Photovoltaic power plants must have the ability to withstand voltage anomalies to a certain extent in order to prevent the loss of power output under grid voltage abnormal conditions.

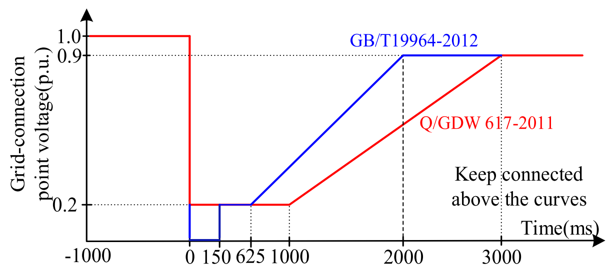

FIGURE 3. Low voltage ride-through requirements for photovoltaic power plants in Chinese grid code specifications [16].

According to the technical regulations of connecting wind farm and photovoltaic power station to power grid, the fault and various disturbances of the power grid must be effectively simulated, especially the grid voltage sag events. Hence, it is meaningful to effectively control the magnitude of frequency fluctuation, the sag depth, the sag duration of power grid voltage and the frequency fluctuations. Thus, the voltage sag generators (VSG) or emulators are urgently needed for this kind of applications. This paper presented a comprehensive overview of voltage sag generators and applications, and it can serve as technical guidelines when choosing a VSG to test the grid adaptivity for the grid-connected inverters and DGs.

The rest of the paper is organized as follows: In the second section, the causes, propagation, classification and hazards of voltage sags are analyzed in details. In section III, four kinds of voltage sag generators (VSGs) are presented and discussed. In section IV, the control and structure of the VSGs based on power electronics converters are briefly introduced. The VSG is classified and discussed according to single-phase, three-phase three-wire and three-phase four-wire systems. Their circuit topology and control diagrams are discussed. Section V introduces the application of VSG in the renewable energy systems. Section VI concludes this paper.

II. CAUSES, PROPAGATION CHARACTERISTICS AND CLASSIFICATION OF VOLTAGE SAG

In this section, the causes, characteristics, propagation and harm of voltage sags are analyzed, which would be described in the following subsections.

A. CAUSES OF VOLTAGE SAG

The main forms of short circuit fault are the single-phase grounding short-circuit, two-phase interphase short-circuit, the two-phase grounding short-circuit and the three-phase grounding short-circuit [17], with a probability of about 70%, 15%, 10%, 5%. In general, the closer to the point of failure, the greater the voltage sag, and the more serious the hazard would be generated for the sensitive electric devices.

B. CHARACTERISTICS OF VOLTAGE SAG

Voltage sag characteristics include the voltage sag amplitude, duration, fault frequency and voltage phase jump. As shown in Fig. 4, ΔU_A, ΔU_B, ΔU_C denotes sag depth, and Δt_a, Δt_b, Δt_c denotes the duration of voltage sag in each phase [18], [19].

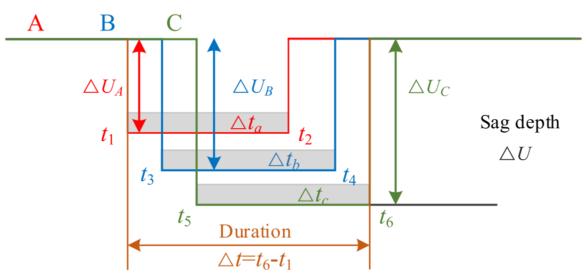

FIGURE 4. Voltage sag illustration in term of sag depth and duration.

The voltage phase jump is mainly caused by the difference between the power system X_S/R_S and the line X_F/R_F ratio, or the voltage imbalance fault occurring in high voltage system is transmitted to the low voltage distribution system through the step-down transformers [20], [21].

As shown in Fig. 5, $Z_s = R_s + jX_s$, $Z_F = R_F + jX_F$, its phase jump angle φ is shown in (1), where a phase jump can be avoided in case of a line failure when $X_s/R_s = X_F/R_F$.

$$\varphi = \arg(\dot{U}_{sag}) = \arctan(\frac{X_F}{R_F}) - \arctan(\frac{X_s + X_F}{R_s + R_F}) \quad (1)$$

where Z_s is the system impedance between (PCC) and power systems, Z_F is the line resistance between PCC and power system, R_F is the system resistance between fault point and PCC, X_S is the line reactance between PCC and power system, X_F is the line reactance between fault point and PCC.

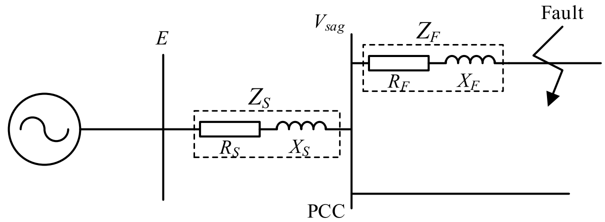

FIGURE 5. Simplified line fault model used for sag analysis [20].

C. PROPAGATION OF VOLTAGE SAG

The voltage sag phenomenon is mainly caused by the short-circuit at nearby or remote electric networks, which includes the symmetrical faults and asymmetrical faults, which can be transformed into different types through transformers.

In Table 1, A~G denotes the type of different kinds of voltage sags, which can be changed into other types when

TABLE 1. Characteristic waveforms and phasor diagram of voltage sag.

Type	Waveform	Phasor Diagram
A	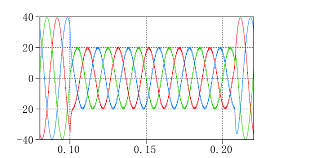	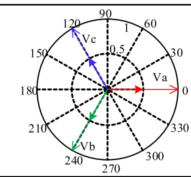
B	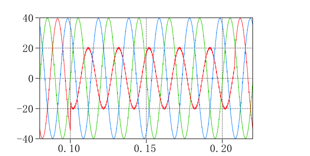	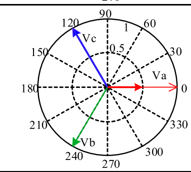
C	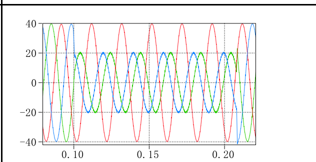	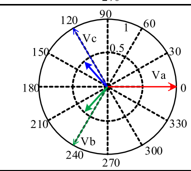
D	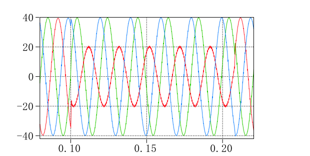	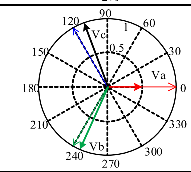
E	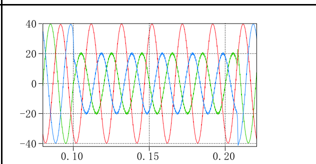	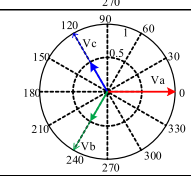
F	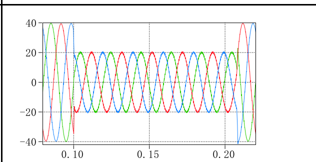	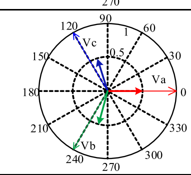
G	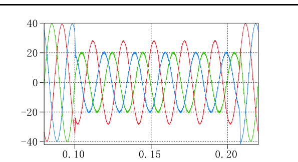	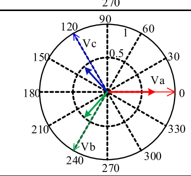

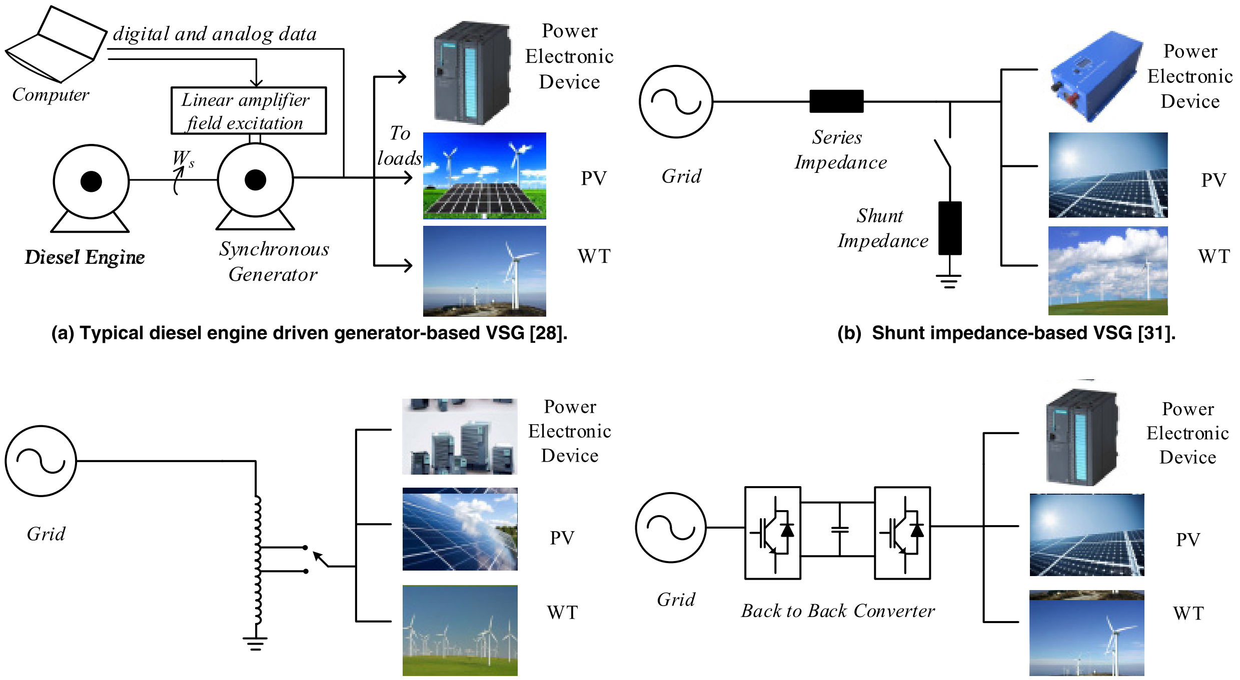

(a) Typical diesel engine driven generator-based VSG [28].

(b) Shunt impedance-based VSG [31].

(c) Transformer based VSG [36]

(d) Full converter-based VSG [37].

FIGURE 6. Four popular voltage sag generator (VSG) schemes in recent literatures [28], [31], [36], [37].

passing through the coupling transformers. The waveforms and phasor diagram are also illustrated in Table 1. Combined with the transfer matrix of transformers and the classification of the sag voltage, the change of the type of voltage sag passing through the coupling transformer can also be easily obtained [19].

D. HARM OF VOLTAGE SAG

Transient power quality problems, such as voltage sags will directly affect or even interrupt the normal power supply of users and cause serious economic losses. This is the most concerned problem for the sensitive customers. Owing to the impact of voltage sags, economic and industrial processes would be damaged, and electrical failures could be generated [22]. Usually, the harm of voltage sag is mainly reflected in the information industry, the large sensitive users and high-tech users, as well as power electronic devices [23]–[25]. At present, research activities in this area can be divided into two aspects: the stability and reliability of the system [26], [27] and the performance improvement of the equipment under various grid voltage sag disturbance conditions.

The voltage sag caused by motor start as mentioned above may have an impact on the adjacent motors and generators. In industry, the occurrence of voltage sag will have a greater impact on the manufacturing process, which is reflected in an increase of product disqualification rate and the economic loss. Any production loss and the subsequent cost caused by voltage sag will lead to great reduction to the product income of the customers. For instance, it will have a huge impact on the semiconductor and integrated chip (IC) manufacturing. And voltage sag also has a great impact on the information industry. It is estimated that more than 45% of data loss and errors on the client side, and more than 80% of server faults appear to be related to voltage sag [21]–[25].

III. REVIEW ON VOLTAGE SAG GENERATOR SCHEMES

As described in IEC 61400-4-11 [18], VSG is a device that can be utilized to simulate voltage sag conditions of power grid in laboratory or field test environment.

In addition, the VSG should be capable of simulating balance and imbalance voltage sag in power grid, and control the depth and duration of voltage sag when simulating power grid. And the controllable voltage recovery curve should also be provided by VSG. According to topologies, there are four types of VSGs [28]–[44], generator-based VSGs [28], shunt impedance-based VSG [29]–[31], transformer-based VSG [32]–[36], and full converter-based VSG [37]–[42]. These popular VSG schemes are briefly summarized in the following subsections, and the advantages and disadvantages of these VSG schemes are also compared and discussed.

A. GENERATOR BASED VSG

This kind of voltage sag generator is a diesel generator with a computer-controlled field excitation circuitry and the data acquisition system, as shown in Fig. 6 (a). The synchronous generator can be controlled to generate the symmetrical voltage sags by changing the field excitation voltage [28].

Field tests show a symmetrical voltage sag can be generated with a rather slow decrease rate of voltage in several periods. Although this method can achieve voltage sag, the response speed is slow and it often takes several cycles to reach the specified depth of the voltage sag.

B. SHUNT IMPEDANCE BASED VSG

In this scheme, the series impedance in the circuit is mainly used to suppress the impact of short-circuit current, and the parallel impedance in the circuit is used to generate voltage sag as shown in Fig. 6 (b). Note that, the ratings of series and shunt impedance can be properly adjusted for high power applications as well [29]–[31]. Since the switching action will introduce harmonic pollution to the system when the voltage drop is realized, the filter circuit needs to be added [31]. Meanwhile, the scheme has the advantages of low cost, easy to realize, but it also has the disadvantages of large energy loss, and the voltage sag cannot be set arbitrarily.

C. TRANSFORMER BASED VSG

Fig. 6 (c) shows the transformer based VSG scheme [36], where the autotransformer is used as the interface for the power electronic switches, in order to achieve instantaneous switching of different turns ratio of the output circuit, so as to simulate the actual voltage rise / fall of the power grid. The switching devices can be relays, three terminal bidirectional silicon controlled devices, IGBTs or contactors. This scheme has the advantages of the fast response, high efficiency and bidirectional energy flow, but the voltage cannot be adjusted automatically.

D. FULL CONVERTER BASED VSG

The most popular solution to build a voltage sag generator is a full converter setup, as shown in Fig. 6 (d). Since the power electronic converters are used to replace the impedances, autotransformers, synchronous generators, thus the volume and weight can be greatly reduced. A systematic overview on this full converter based VSG scheme would be discussed in the following section [37]–[44].

IV. OVERVIEW ON FULL INVERTER BASED VSG

In this part, the full inverter-based VSG is discussed for the application in the single-phase, three-phase three-wire and three-phase four-wire electric power systems. Advantages and disadvantages of these schemes are also presented in the following [45]–[60].

A. SINGLE-PHASE INVERTER BASED VSG

In this scheme, single-phase H-bridge inverters are used as independent control units to realize complete decoupling of VSG three-phase outputs, and then to simulate the arbitrary waveforms of power network faults.

In [45], a voltage sag control strategy for the balanced and unbalanced three-phase voltage sag generator (VSG) and the electrical equipment test is presented. The three single-phase inverters and unipolar PWM scheme with simple structure was applied. Based on the unipolar modulation method, the pulse width modulation (PWM) technique is used to control each inverter, as shown in Fig. 7.

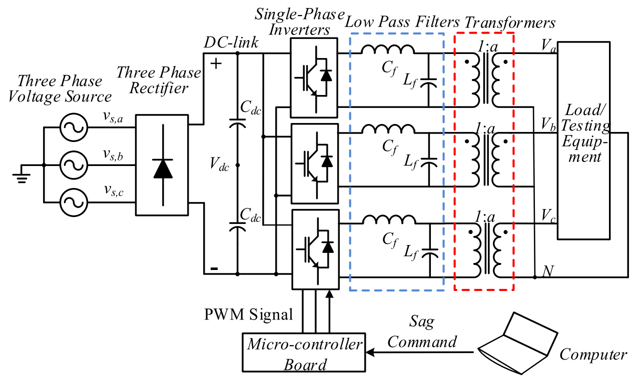

FIGURE 7. Circuit diagram of the balanced and unbalanced voltage sag generator [45].

The three single-phase H-bridge inverters are connected to the common DC link to convert DC voltage to AC voltage. Two kinds of voltage sags, i.e., Type-A and Type-B, can be generated by using this scheme, which has an advantages of a simple control strategy, complete decoupling of the three-phase output signals, and simple circuit topology. However, since this topology adopts three single-phase H-bridge inverters, the independent LC low-pass filters and Y-type transformers are needed for each phase, and its volume and the number of power electronic devices are relatively large and expensive.

B. BACK-TO-BACK INVERTER BASED VSG

This scheme is the most popular application scheme at present. The main circuit topology of the VSG system is constructed by two three-phase voltage source converters through a fully symmetrical "back-to-back" (BTB) connection, which is used to simulate the power output characteristics of the infinite grid under normal and various fault conditions.

The scheme is characterized by dividing VSG into two parts to control, namely, the front circuit and the fault generation side circuit, as shown in Fig. 8 (a) [46]. The front-end circuit is mainly controlled by improved voltage and current double closed-loop SPWM to control DC bus voltage and keep it stable as shown in Fig.8(b). By effectively controlling the magnitude and frequency of the output voltage of each phase, various symmetrical and asymmetrical voltage sag, over-voltage, flicker and other grid disturbances can be simulated. The three-phase voltage phasor relationship among various power grid faults is illustrated in Fig.9.

As shown in Fig. 9, the phase voltages can be expressed as $\dot{U}_a$, $\dot{U}_b$, $\dot{U}_c$ and $\dot{U}_{ab}$, $\dot{U}_{bc}$, $\dot{U}_{ca}$ denote line voltages, dotted lines are expressed as symmetrical phasor relations of three-phase voltages, and solid lines expressed as asymmetrical phasor relations of the three-phase voltages. When a three-phase symmetrical voltage sag occurs, the voltage of each phase decreases to the original p (0-1.2) times, and the

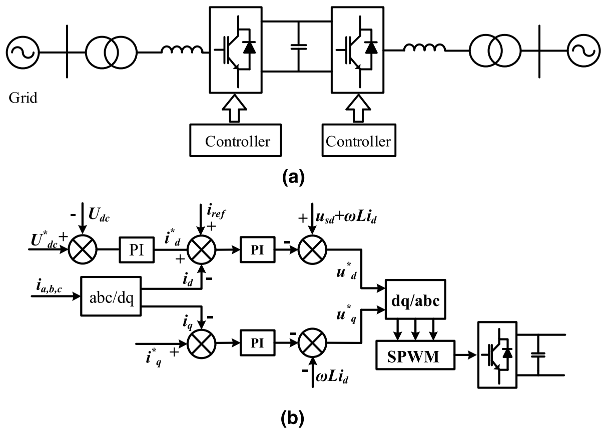

FIGURE 8. (a). Structure diagram of back-to-back VSG system (b). Control block diagram of grid-side converter [46].

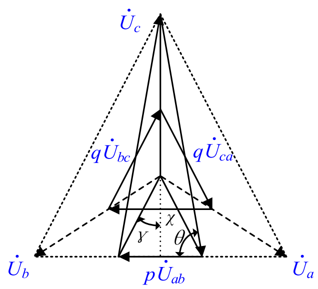

FIGURE 9. Three-phase voltage phase diagram [46]. *where θ is the angle of line voltage; γ and χ are the angle and amplitude of phase a and b voltage to neutral point respectively; U' is the effective value of line voltage. p and q are the multiples of voltage sag in amplitude.

phase angles remain unchanged, as shown by the dotted line. The voltage sag of phase A and B is shown in (2) and (3).

$$\begin{cases} \theta = \operatorname{atan}\left(\dfrac{\sqrt{3}}{p}\right) \\ \gamma = \operatorname{atan}\left(\sqrt{3}p\right) \\ \chi = \dfrac{pU'}{2\sin\left(\operatorname{atan}\left(\sqrt{3}p\right)\right)} \\ q = \dfrac{p}{2\cos\left(\operatorname{atan}\left(\dfrac{\sqrt{3}}{p}\right)\right)} \end{cases} \tag{2}$$

$$\begin{cases} u_a(t) = \sqrt{\dfrac{2}{3}}pU'\sin(2\pi ft) \\ u_b(t) = \sqrt{\dfrac{2}{3}}qU'\sin(2\pi ft + \pi - \theta) \\ u_c(t) = \sqrt{\dfrac{2}{3}}qU'\sin(2\pi ft - \pi + \theta) \end{cases} \tag{3}$$

When the amplitude and phase of $\dot{U}_c$ remain unchanged, and $\dot{U}_{ab}$ falls to the original p-fold. In order to maintain the neutral point balance, $\dot{U}_{bc}$ and $\dot{U}_{ca}$ get a fall to the original q-fold. As shown in Fig. 9, formula (2) can be obtained according to voltage vector relation and Kirchhoff's law. According to (2), three-phase fault voltage can be obtained as (3). In the normal state, $p = q = 1$, $\theta = 2\text{pi}/3$. Various voltage sags can be simulated by (3) in case of voltage sags.

In [47], a three-phase voltage transient simulation system is proposed and discussed. And a non-external power supply topology is adopted and the control loop in each phase is fed in the system. As shown in Fig. 10, voltage transients can be generated by adding an AC signal in series in each phase. In the aspect of control, a time-varying three-phase system is converted into two non-variable systems [48] by using Park and Clark transformation.

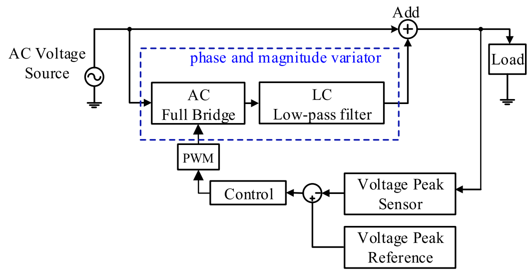

FIGURE 10. Single-loop topology with converters and transformers [47].

C. THREE-PHASE FOUR-WIRE INVERTER BASED VSG

A dc bus split capacitor inverting circuit is proposed in [20]. The neutral point of the DC bus split capacitor is taken as the output neutral line, so that the original three-phase three-wire system is transformed into three-phase four-wire system to realize a complete decoupling of output voltages [50], [51].

The structure diagram of the split-capacitor inverter-based voltage sag generator is shown in Fig. 11 (a), and the pertinent control strategy is given in Fig. 11 (b). The reference values of the output voltages of each phase can be obtained by vector transformation through given fault type, amplitude of rise/fall, duration of fault and other parameters, which can be used as reference value of the external voltage loop.

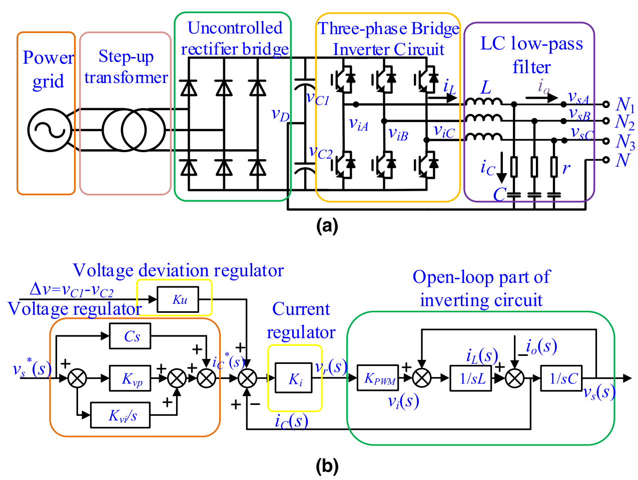

FIGURE 11. (a). Control diagram of split-capacitor inverter-based VSG. (b). Topology of split-capacitor inverter-based VSG [20].

TABLE 2. Comparison of several VSG schemes in recent literatures [28]–[42].

Classification of VSG	Application of LVRT test devices in renewable energy systems (RESs)	Recommendation level
Generator based VSG [28]	• Only three-phase symmetrical voltage sag is produced. • The device is large in volume.	Not recommended
Shunt impedance based VSG [29-31]	• The structure of the topology is simple, and the control scheme is easy to implement. • Voltage sag depth is difficult to be controlled accurately. • The function of reactive power regulation cannot be comprehended.	☆☆
Transformer based VSG [32-36]	• Power rating is high, the volume and weight are large and it is not portable. • Compared with the impedance type VSG, the power loss is rather small, and its structure is simple and is easy to achieve. Moreover, if the ratio of transformer is adjustable, the depth of voltage sag can also be easily adjusted.	☆☆☆
Full converter based VSG [37-42]	• The weight of VSG is remarkably reduced, which is preferred for field testing. • The cost is high, the control is complex and the reliability would be highly dependent on power devices. • The ability to resist voltage and current overloads under power grid failure is limited.	☆☆☆

The PI controller is used to the outer voltage loop. The sum of output value and voltage deviation value of the split capacitor of the DC bus is taken as the input reference value of the current inner loop.

Since the three-phase voltages are controlled independently, after the three single-phase modulation signals are combined, all the control signals are generated by SPWM modulation module, and then the output voltage of each phase of VSG can be controlled. In [52], the simulation and experiment of three-phase four-wire VSG based on three-dimensional space vector modulation (SVPWM) [52], [53] in *abc* algorithm is introduced and the experimental results have been provided for validation.

On the other hand, in recent works, the matrix converter (MC) has been extensively studied [54]–[57]. A 3-phase 4-leg matrix converter with 12 switches is shown in Fig. 12. By controlling the turn-on or turn-off sequences of switches in the matrix converter, the conversion of an arbitrary phase, amplitude and frequency can be realized [55], [58], [59].

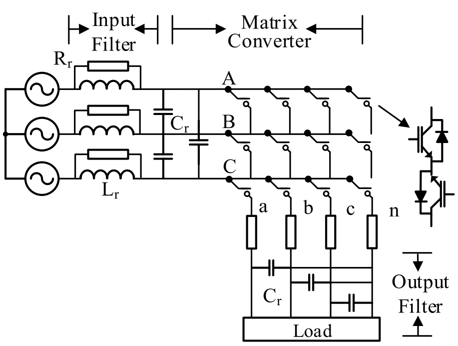

FIGURE 12. VSG diagram based on matrix converter topology [55].

The same disadvantage exists in the synthesized unbalanced voltage sag of the matrix converters [55], [56], [57]. For matrix converters or back-to-back (BTB) converter, owing to the requirement for three-dimensional space-vector modulation (3V-SVPWM) algorithm, the control would be more complex when three-phase four-wire system is tested [55].

The four kinds of VSG when used in RES systems are compared in Table 2. At present, the generator based VSG is out of use for its poor performance. Impedance based VSG can be applied in low cost applications. Power electronic converter based VSG is widely concerned due to the powerful functions. Transformer based VSG is simple in structure, and has high reliability and low cost. With the development of high-power rating power electronic devices and the reduction of their cost, the power electronic converter based VSG will be widely applied due to its small size, portability and powerful functions.

V. APPLICATION OF VOLTAGE SAG GENERATOR IN RENEWABLE ENERGY SYSTEM

In this part, several application schemes of VSG in RES are briefly presented, which can be widely utilized in the practical applications.

A. LVRT TESTING OF GRID-CONNECTED PV SYSTEM

In order to test the LVRT capabilities of wind turbines and photovoltaic power generation equipment [49], [61]–[64], it is necessary to simulate various fault phenomena of power grid, especially, the voltage sag phenomenon. In [62], an entire design of PV system built on real time digital simulator (RTDS) including the PV array with maximum power point tracking (MPPT) capability is presented. The voltage sag of power grid from 90% to 0% can be simulated and good performance has been obtained by this method.

Only sag of one degree can be realized by the traditional impedance type VSG if the value of the resistance group or reactor group is fixed. In [62], a novel topology is presented, which consists of reactors of fixed value but its equivalent impedance value can be changed by breakers parallel or shunt connected in circuit as shown in Fig. 13.

B. LVRT TESTING OF WIND POWER GENERATION SYSTEM

The development and utilization of wind energy has received increasing attention throughout the world. The LVRT test of wind power generators is of vital significance. Two existing

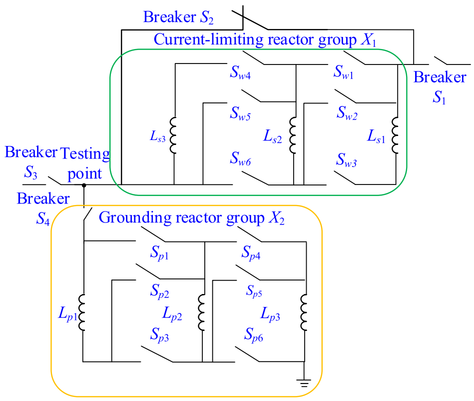

FIGURE 13. Topology of LVRT device for grid-connected PV system [62].

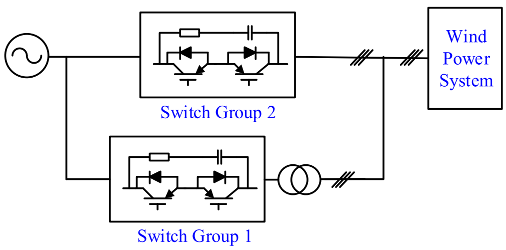

FIGURE 14. Topology of VSG proposed in [37].

voltage sag generators: variable transformer based and back-to-back VSG are discussed and compared in [26].

As shown in Fig. 14, there are two switches groups for the three-phase system, where each switch group consists of three bidirectional switches for each phase. Then, a step-down transformer is inserted into the branch of the switch group 1. By switching the switch group, the conversion between failure mode and normal mode can be realized.

C. WIND GENERATOR GRID ADAPTABILITY TESTING DEVICE

The wind turbine grid adaptability testing device consists of two back-to-back (BTB) modular multilevel converters [65],

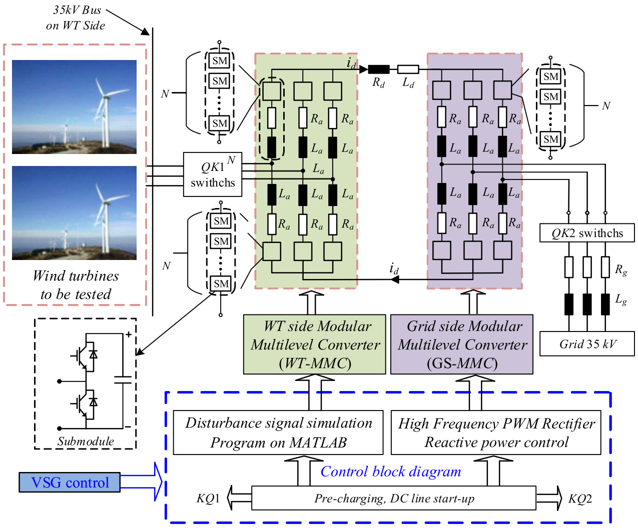

FIGURE 15. Wind power generation system grid adaptability testing device and its control block diagram [65].

the DC charging startup module, and disturbance generation module, which is directly connected to 35 kV bus of the wind power system, is shown in Fig. 15. By using this scheme, various grid disturbances can be flexibly simulated to test the grid adaptivity of the wind power generation system.

Furthermore, the real-time digital simulation platform, a closed-loop detection platform for converter controller of the permanent magnet synchronous generator (PMSG) set is built based on the actual controller of a wind turbine and BTB converters, as shown in Fig. 16. RTDS outputs the required wind turbine speed, position, rotor/stator current, grid voltage, DC voltage and other signals to the controller through the A/O ports and amplifiers. The main controller of the converter of the wind power generation system forms a real-time control strategy based on the collected electrical parameters, and then receives the dual PWM pulse signal and

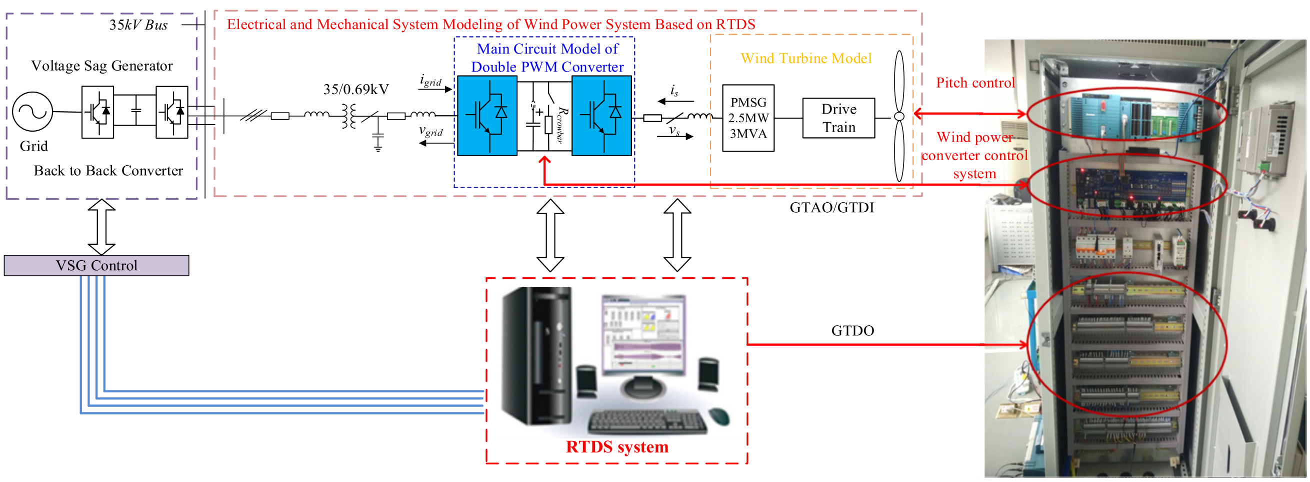

FIGURE 16. Electrical and mechanical system equivalent modeling of wind power generation system based on RTDS and DSP based controllers.

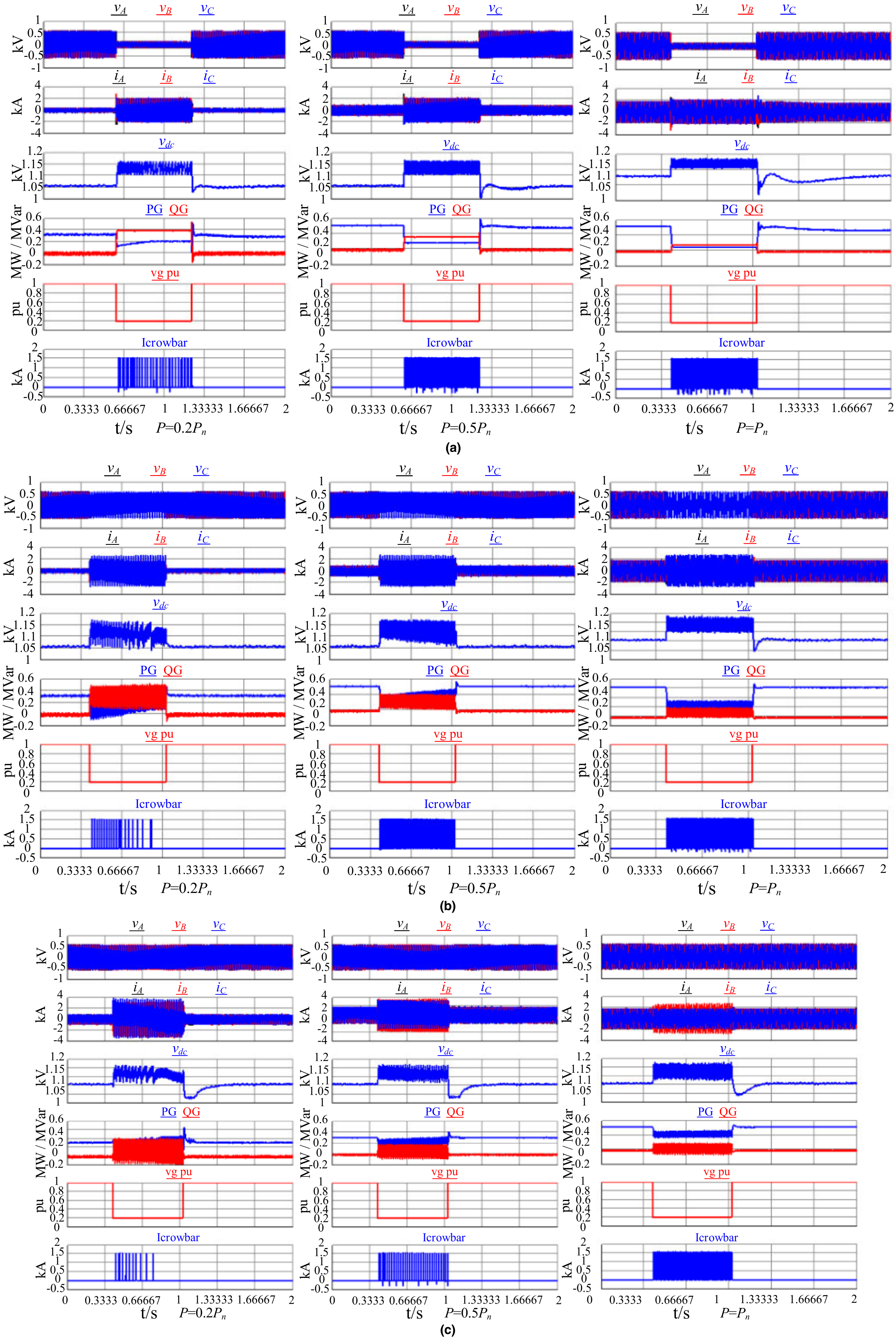

FIGURE 17. Dynamic waveforms of electrical parameters on WT side when voltage drop to 20% Un. (a) Three-phase voltage sag occurs at grid-connection points. (b) Two-phase voltage sag occurs at grid-connection points(c) Single-phase voltage sag occurs at grid-connection points.

pitch angle from the controller through the DI port of RTDS. Noteworthy, only wind turbine and dual PWM converters use the DSP controller, and the rest of the main circuit, VSG system, etc., are realized by using RTDS simulation models. Notably, the VSG model can be realized by any back-to-back converter topology, such as the three-level converter, or modular multilevel converter based circuit architecture, using the RSCAD based real-time simulation algorithms in the RTDS platform. Besides, the wind power generator parameters are shown in Table 3.

TABLE 3. Generator parameters of the studied wind power generator.

Parameters	Value	Parameters	Value
Rated power	1611kW	Polar logarithm	40
Rated voltage	690V	Straight-axis inductance Ld	1.4353mH
Power factor	0.9248	Quadrature inductance Lq	1.4273mH
Rated current	1457.6A	Stator resistance Rs	0.0081Ω
Rated speed	16.6 rpm	Rotor flux linkage	8.1Wb
Connect mode	Y/△	Short circuit impedance	5%

The processor allocation of real-time simulation system is optimized by combining the large step size model with the small step size model. The simulation step of the small step model is about 2-5 μs, the simulation step of the large step model is about 50 μs. The small step model mainly includes the wind turbine model and the main circuit model of the BTB converter. The large step model mainly includes the power part model (wind speed, wind turbine, transmission system, pitch angle actuator), the power network model and the signal feedback module needed for the closed-loop detection. The small step model is connected to the main network system by the interface transformer.

During the LVRT testing, symmetrical and asymmetrical voltages in different sag depth and duration can be generated. In this experiment, three different voltage sags, A, B and E, were produced by controlling VSG to achieve the effect of voltage faults at the grid-connected points. The depth and duration of the voltage sags were 20% and 0.6s. The dynamic changes of electrical parameters are shown in Fig. 17.

Fig. 17 (a) presents the dynamic waveforms of electrical parameters on the WT side when a three-phase symmetrical voltage sag occurs at grid-connection points. The voltage sag of 20% depth occurs at $t = 0.6$ seconds, and the voltage is restored to the rated voltage at $t = 1.2$ seconds. During this period, the current of each phase increases, the voltage of DC bus increase to 1.18kV peak value and reactive power increases to 0.4 MVar, active power decreases to 0.2 MW, and the current through $r_{crowbar}$ increases to 1.5kA.

Fig.17 (b) shows the dynamic waveforms of electrical parameters on wind power generator when the two-phase voltage sag occurs at the grid-connection points. A temporary voltage sag of phase A and phase B in 20% depth occurs at $t = 0.6$ seconds, and the voltage is restored to the rated voltage at $t = 1.2$ seconds. During this period, the current of each phase increases while phase C increases more, the voltage of DC bus increases to 1.18kV, and the reactive power increases to 0.5MW, active power decreases to 0.18 MVar, and current through $r_{crowbar}$ increases to 1.5kA eventually.

The dynamic waveforms of the electrical parameters on WT side when single-phase voltage sag occurs at grid-connection points are presented in Fig.17 (c). A temporary voltage sag of phase A in 20% depth occurs at $t = 0.6$ seconds, and the voltage is restored to the rated voltage at t = 1.2 seconds. During this period, the current of each phase increases while phase B and C increases more, the voltage of DC bus increases to 1.17kV peak value, reactive power increases to 0.2 MVar, active power decreases to 0.1 MW, and $i_{crowbar}$ increase to 1.5kA.

In retrospect, a comparative study of dynamic responses of three and four wind turbines to voltage sags and swells was given in [66], taking into account both the symmetrical and asymmetrical voltage sags and voltage surges. And the effects of symmetrical and asymmetrical voltage sags on the doubly fed induction generator (DFIG)-based wind turbines was studied in [67]. The influence of voltage sag on DFIG wind power system by combining theoretical analysis with simulation was discussed in [68]. Then, the transient process of crowbar-based wind power system [69], [70] during fault was simulated and analyzed. The transient overcurrent of the rotor during the voltage sag period could be suppressed to maintain the uninterrupted operation of the system, and some reactive power support could be provided to the grid during the fault recovery period to assist the grid voltage recovery.

VI. CONCLUSION

This paper presents an overview of voltage sag generator and its application in RES. Firstly, the harm, characteristics, causes and propagation of voltage sag are presented. The four kinds of VSG are compared, which include generator-based VSG, shunt impedance-based VSG, transformer-based VSG, and full converter-based VSG.

The single-phase scheme has the advantages of relatively simple control strategy, complete decoupling of three-phase output, simple topology and enhanced stability properties. However, the hardware volume and the number of various power electronic devices are large, and the cost of equipment is high. As the three-phase output voltages of the three-phase scheme is coupled with each other, it is impossible to realize independent control of arbitrary phase voltage, and then it is impossible to fully simulate all kinds of fault waveforms in power system. Therefore, when simulating the pure single-phase voltage sag/swell faults, the voltage waveforms of the non-fault phases will inevitably change in the amplitude and phase. On the other hand, the three-phase four-wire topology can realize a complete decoupling among the three-phase variables, but it also has complex control strategies.

In addition, the matrix converter has become one of the research mainstreams of the power electronics area, and has a wide range of application prospect. In actual system testing, the choice of VSG can be considered comprehensively according to the requirements of power grid rules, such as fault types that need to be simulated, and system volume, weight, and cost. The full converter-based VSG are the mainstream recently, however, in LVRT test of renewable energy systems, the group reactance and transformer based approaches can still be widely used owing to the low cost and control simplicity.

Finally, a case study of LVRT testing facility is discussed, based on our recent research project, where a closed-loop detection platform is built based on the actual controller of wind turbine on RTDS platform for grid adaptability test. The VSG devices can be widely applied for LVRT and grid adaptability studies for various types of RESs.

REFERENCES

[1] X. Wang and F. Blaabjerg, "Harmonic stability in power electronic–based power systems: Concept, modeling, and analysis," *IEEE Trans. Smart Grid*, vol. 10, no. 3, pp. 2858–2870, May 2019.

[2] F. Blaabjerg, Z. Chen, and S. Kjaer, "Power electronics as efficient interface in dispersed power generation systems," *IEEE Trans. Power Electron.*, vol. 19, no. 5, pp. 1184–1194, Sep. 2004.

[3] C. Wang, X. Yang, Z. Wu, Y. Che, L. Guo, S. Zhang, and Y. Liu, "A highly integrated and reconfigurable microgrid testbed with hybrid distributed energy sources," *IEEE Trans. Smart Grid*, vol. 7, no. 1, pp. 451–459, Jan. 2016.

[4] Q.-C. Zhong, "Virtual synchronous machines: A unified interface for grid integration," *IEEE Power Electron. Mag.*, vol. 3, no. 4, pp. 18–27, Dec. 2016.

[5] J. Rocabert, A. Luna, F. Blaabjerg, and P. Rodríguez, "Control of power converters in AC microgrids," *IEEE Trans. Power Electron.*, vol. 27, no. 11, pp. 4734–4749, Nov. 2012.

[6] Y. Zhou and C. N.-M. Ho, "A review on microgrid architectures and control methods," in *Proc. IEEE 8th Int. Power Electron. Motion Control Conf. (IPEMC-ECCE Asia)*, May 2016, pp. 3149–3156.

[7] Z. Jin, M. Hou, F. Dong, and Y. Li, "A new control strategy of dc microgrid with photovoltaic generation and hybrid energy storage," in *Proc. IEEE PES Asia–Pacific Power Energy Eng. Conf. (APPEEC)*, Oct. 2016, pp. 434–438.

[8] *IEEE Approved Draft Recommended Practice for Voltage Sag and Interruption Ride-Through Testing for End Use Electrical Equipment Less than 1,000 Volts*, IEEE Standard P1668/D4Q, May 2014, pp. 1–103.

[9] J. Lucio, E. Espinosa-Juárez, and A. Hernández, "Voltage sag state estimation in power systems by applying genetic algorithms," *IET Gener. Transm. Distrib.*, vol. 5, no. 2, p. 223, 2011.

[10] R. Naidoo and P. Pillay, "A new method of voltage sag and swell detection," *IEEE Trans. Power Del.*, vol. 22, no. 2, pp. 1056–1063, Apr. 2007.

[11] *IEEE Draft Recommended Practice for Monitoring Electric Power Quality*, IEEE Standard P1159/D6, Jan. 2019, pp. 1–104.

[12] J. Gomez and M. Morcos, "Voltage sag and recovery time in repetitive events," *IEEE Trans. Power Del.*, vol. 17, no. 4, pp. 1037–1043, Oct. 2002.

[13] O. S. Senturk and A. M. Hava, "A simple sag generator using SSRs," *IEEE Trans. Ind. Appl.*, vol. 48, no. 1, pp. 172–180, Jan. 2012.

[14] W. S. Wang, Y. Chi, Z. Zhang, and Y. Li, *Standard on Connecting Wind Farms to Power System*, Standard GB/T 19963-2011, (in Chinese), China Standardization, Mar./Apr. 2016, pp. 86–89.

[15] C. Liu, W. Shi, and H. Zhao, "Comparison of China's wind power integration standard with similar foreign standards," (in Chinese), *Smart Grid*, vol. 2, no. 9, pp. 48–51, 2014.

[16] Z. Cao, S. Zhao, X. Wei, and Z. Yuan, "Comparison between domestic and international standards grid connection techniques of PV power station," (in Chinese), *Electr. Power Survey Des.*, no. 6, pp. 65–69, 2017.

[17] M. Bollen, "Characterisation of voltage sags experienced by three-phase adjustable-speed drives," *IEEE Trans. Power Del.*, vol. 12, no. 4, pp. 1666–1671, Oct. 1997.

[18] *Electromegnetic Compatibility (EMC)—Part 4-11: Testing and Measurement Electomegnetic Compatibility (EMC)—Part 4-11: Testing and Measurement Techniques Voltage Dips, Short Interruptions and Voltage Variations Immunity Tests*, IEC Standard 61000-4-11, 2004.

[19] C. Wang, "Typical characteristic quantity analysis and propagation characteristics study of voltage sag," (in Chinese), M.S. thesis, Zhengzhou Univ., Zhengzhou, China, 2019.

[20] X. Du, "Research on control strategy and realization of voltage sag generator," (in Chinese), M.S. thesis, North China Electr. Power Univ., Beijing, China, Mar. 2014.

[21] V. E. Wagner, A. A. Andreshak, and J. P. Staniak, "Power quality and factory automation," *IEEE Trans. Ind. Appl.*, vol. 26, no. 4, pp. 620–626, Jul./Aug. 1990.

[22] A. Polycarpou, H. Nouri, T. Davies, and R. Ciric, "An overview of voltage sag theory, effects and equipment compatibility," in *Proc. 39th Int. Universities Power Eng. Conf. (UPEC)*, Sep. 2004, pp. 966–972.

[23] P. K. Lim and D. S. Dorr, "Understanding and resolving voltage sag related problems for sensitive industrial customers," in *Proc. IEEE Power Eng. Soc. Winter Meeting Conf. Proc.*, Jan. 2000, pp. 2886–2890.

[24] E. R. Collins and M. A. Bridgwood, "The impact of power system disturbances on AC-coil contactors," in *Proc. IEEE Annu. Textile, Fiber Film Ind. Tech. Conf.*, May 1997, pp. 1–6.

[25] N. K. Medora, A. Kusko, and M. Thompson, "Impact of line voltage sag on switch mode power supply operation," in *Proc. 3rd IEEE Conf. Ind. Electron. Appl.*, Jun. 2008, pp. 2178–2183.

[26] C. He, F. Li, and V. K. Sood, "Static transfer switch (STS) model in EMTPWorks RV," in *Proc. Can. Conf. Elect. Comput. Eng.*, vol. 1, 2004, pp. 111–116.

[27] Y. Zhiyong, L. Guangbin, and W. Hong, "Development of generator for voltage dips, short interruptions and voltage variations immunity test," in *Proc. 3rd Int. Symp. Electromagn. Compat.*, May 2002, pp. 67–70.

[28] E. Collins and R. Morgan, "A three-phase sag generator for testing industrial equipment," *IEEE Trans. Power Del.*, vol. 11, no. 1, pp. 526–532, Jan. 1996.

[29] M. García-Gracia, M. Paz Comech, J. Sallán, D. López-Andía, and O. Alonso, "Voltage dip generator for wind energy systems up to 5 MW," *Appl. Energy*, vol. 86, no. 4, pp. 565–574, Apr. 2009.

[30] S. Hu, J. Li, and H. Xu, "Comparison of voltage sag generators for wind power system," in *Proc. Asia–Pacific Power Energy Eng. Conf.*, Mar. 2009, pp. 1–4.

[31] I. J. Gabe, H. A. Grundling, and H. Pinheiro, "Design of a voltage sag generator based on impedance switching," in *Proc. IECON*, Nov. 2011, pp. 3140–3145

[32] Y. Kumsuwan, C. Boonmee, and S. Premrudeepreechacharn, "Implementation of a 1-kVA programmable balanced three-phase voltage sag generator," in *Proc. 6th Int. Conf. Elect. Eng./Electron., Comput., Telecommun. Inf. Technol.*, vol. 1, 2009, pp. 46–49.

[33] Y. Ma and G. G. Karady, "A single-phase voltage sag generator for testing electrical equipments," in *Proc. IEEE/PES Transmiss. Distrib. Conf. Expo.*, Apr. 2008, pp. 1–5.

[34] A. O. Ibrahim, T. H. Nguyen, D.-C. Lee, and S.-C. Kim, "Ride-through strategy for DFIG wind turbine systems using dynamic voltage restorers," in *Proc. IEEE Energy Convers. Congr. Expo.*, Sep. 2009, pp. 1611–1618.

[35] J. G. Nielsen, M. Newman, H. Nielsen, and F. Blaabjerg, "Control and testing of a dynamic voltage restorer (DVR) at medium voltage level," in *Proc. IEEE 34th Annu. Conf. Power Electron. Spec. (PESC)*, vol. 3, Jun. 2003, pp. 1248–1253.

[36] C. Wessels, R. Lohde, and F. W. Fuchs, "Transformer based voltage sag generator to perform LVRT and HVRT tests in the laboratory," in *Proc. 14th Int. Power Electron. Motion Control Conf. (EPE-PEMC)*, 2010, pp. T11-8–T11-13.

[37] L. Dongyu, Z. Honglin, X. Shuai, and Y. Geng, "A new voltage sag generator base on power electronic devices," in *Proc. 2nd Int. Symp. Power Electron. Distrib. Gener. Syst.*, Jun. 2010, pp. 584–588.

[38] M. Yamada, A. Iwata, J. Okada, Y. Hatakeyama, and Y. Ishii, "A new voltage sag compensator with a gradationally controlled voltage inverter," in *Proc. Eur. Conf. Power Electron. Appl.*, 2005, pp. 1–7.

[39] R. Lohde and F. W. Fuchs, "Laboratory type PWM grid emulator for generating disturbed voltages for testing grid connected devices," in *Proc. 13th Eur. Conf. Power Electron. Appl.*, 2009, pp. 1–9.

[40] S. A. Richter, J. Von Bloh, C. P. Dick, D. Hirschmann, and R. W. De Doncker, "Control of a medium-voltage test generator," in *Proc. IEEE Power Electron. Spec. Conf.*, Jun. 2008, pp. 3787–3793.

[41] C. Saniter and J. Janning, "Test bench for grid code simulations for multi-MW wind turbines, design and control," *IEEE Trans. Power Electron.*, vol. 23, no. 4, pp. 1707–1715, Jul. 2008.
[42] Y. Chung, G. Kwon, T. Park, and K. Lim, "Voltage sag and swell generator for the evaluation of custom power devices," in *Proc. IEEE Power Eng. Soc. General Meeting*, vol. 4, Jun. 2004, pp. 2503–2507.
[43] S. Dokic, J. Milanovic, and K. Charalambous, "Computer simulation of voltage sag generator," in *Proc. 10th Int. Conf. Harmon. Qual. Power.*, vol. 2, Mar. 2004, pp. 649–654.
[44] C. Boonmee, Y. Kumsuwa, and S. Premrudeepreechacharn, "Implementation of real time three phase balanced voltage sag generator 1 kVA: Using microcontroller and PC control," in *Proc. ICCAS-SICE*, 2009, pp. 903–907.
[45] K. Daychosawang and Y. Kumsuwan, "Balanced and unbalanced three-phase voltage sag generator for testing electrical equipment," in *Proc. 11th Int. Conf. Electr. Eng./Electron., Comput., Telecommun. Inf. Technol. (ECTI-CON)*, May 2014, pp. 1–6.
[46] X. Wang, "Study on the multi-mode voltage swell/sag generator (VSSG) based on the IGBT PWM control," (in Chinese), M.S. thesis, Hangzhou Dianzi Univ., Hangzhou, China, Mar. 2017.
[47] J. Caicedo and J. Posada, "Three-phase voltage transients emulator," in *Proc. 6th IEEE Conf. Ind. Electron. Appl.*, Jun. 2011, pp. 2563–2568.
[48] D.-C. Lee and D.-S. Lim, "AC voltage and current sensorless control of three-phase PWM rectifiers," in *Proc. IEEE 31st Annu. Power Electron. Spec. Conf.*, vol. 2, Jun. 2000, pp. 588–593.
[49] J. Morren and S. W. H. de Haan, "Ridethrough of wind turbines with doubly-fed induction generator during a voltage dip," *IEEE Trans. Energy Convers.*, vol. 20, no. 2, pp. 435–441, Jun. 2005.
[50] W. Muangjai, S. Premrudeepreechacharn, K. Higuchi, K. Oranpiroj, and W. Jantee, "An implementation algorithm of a carrier-based PWM technique for three-phase four-leg voltage sag generator with microcontroller," in *Proc. IEEE 10th Int. Conf. Power Electron. Drive Syst. (PEDS)*, Apr. 2013, pp. 852–855.
[51] K. Oranpiroj, S. Premrudeepreechacharn, M. Ngoudech, W. Muangjai, K. Yingkayun, and T. Boonsai, "The 3-phase 4-wire voltage sag generator based on three dimensions space vector modulation in abc coordinates," in *Proc. IEEE Int. Symp. Ind. Electron.*, Jul. 2009, pp. 275–280.
[52] R. Wu, D. Chen, and S. Xie, "A three-dimensional space vector modulation algorithm in a-b-c coordinate implemented by a FPGA," in *Proc. 31st Annu. Conf. IEEE Ind. Electron. Soc. (IECON)*, 2005, pp. 1071–1075.
[53] W. Rui and X. Shaojun, "Research of the four-leg voltage source inverters based on space vector modulation in abc coordinates," in *Proc. Int. Conf. Elect. Mach. Syst.*, vol. 2, 2005, pp. 1442–1446.
[54] P. W. Wheeler, J. C. Clare, M. Apap, D. Lampard, S. J. Pickering, K. J. Bradley, and L. Empringham, "An integrated 30kw matrix converter based induction motor drive," in *Proc. IEEE 36th Power Electron. Spec. Conf.*, Jun. 2005, pp. 2390–2395.
[55] R. Cardenas, C. Juri, R. Pena, J. Clare, and P. Wheeler, "Analysis and experimental validation of control systems for four-leg matrix converter applications," *IEEE Trans. Ind. Electron.*, vol. 59, no. 1, pp. 141–153, Jan. 2012.
[56] R. Cárdenas, R. Peña, P. Wheeler, and J. Clare, "Resonant controllers for 4-leg matrix converters," in *Proc. IEEE Int. Symp. Ind. Electron.*, Jul. 2010, pp. 1027–1032.
[57] X. Lie and X. Hanwei, "Analysis of common mode voltage for a four-leg matrix converter," (in Chinese), in *Proc. IEEE Transp. Electrific. Conf. Expo, Asia–Pacific (ITEC Asia–Pacific)*, Aug. 2017, pp. 1–6.
[58] M. Díaz and R. Cárdenas, "Matrix converter based voltage sag generator to test LVRT capability in renewable energy systems," in *Proc. 8th Int. Conf. Exhib. Ecological Vehicles Renew. Energies (EVER)*, 2013, pp. 1–7.
[59] W. Jantee, S. Premrudeepreechacharn, K. Oranpiroj, and W. Muangjai, "Voltage sag signal generator program for testing electrical equipment," in *Proc. Int. Electr. Eng. Congr. (iEECON)*, 2014, pp. 1–4.
[60] R. Cardenas, R. Pena, M. Perez, J. Clare, G. Asher, and F. Vargas, "Vector control of front-end converters for variable-speed wind–diesel systems," *IEEE Trans. Ind. Electron.*, vol. 53, no. 4, pp. 1127–1136, Jun. 2006.
[61] M. Inci, T. Demirdelen, A. Tan, T. Köroglu, M. U. Cuma, K. Ç. Bayindir, and M. Tümay, "A novel low cost sag/swell generator," in *Proc. IEEE 6th Int. Symp. Power Electron. Distrib. Gener. Syst. (PEDG)*, Jun. 2015, pp. 1–4.
[62] Z. Fei, Z. Junjun, and D. Mingchang, "A novel voltage sag generator for low voltage ride-through testing of grid-connected PV system," in *Proc. IEEE Int. Conf. Comput. Sci. Automat. Eng. (CSAE)*, vol. 2, May 2012, pp. 136–140.
[63] O. Abdel-Baqi and A. Nasiri, "A dynamic LVRT solution for doubly-fed induction generator," *IEEE Trans. Power Electron.*, vol. 25, no. 1, pp. 193–196, Jan. 2010.
[64] F. Lima, A. Luna, P. Rodriguez, E. Watanabe, and F. Blaabjerg, "Rotor voltage dynamics in the doubly fed induction generator during grid faults," *IEEE Trans. Power Electron.*, vol. 25, no. 1, pp. 118–130, Jan. 2010.
[65] Y. Han, "Wind turbine grid adaptability testing device and testing method," (in Chinese), China Patent 103 969 578 B, Mar. 2014.
[66] T. K. Das, J. Zhang, and H. R. Pota, "Comparative study of the response of wind turbine generators to voltage sags and swells," in *Proc. Australas. Universities Power Eng. Conf. (AUPEC)*, Sep. 2016, pp. 1–6.
[67] M. Mohseni, S. M. Islam, and M. A. S. Masoum, "Impacts of symmetrical and asymmetrical voltage sags on DFIG-based wind turbines considering phase-angle jump, voltage recovery, and sag parameters," *IEEE Trans. Power Electron.*, vol. 26, no. 5, pp. 1587–1598, May 2011.
[68] F. Liu, M. Mei, and J. Pan, "A control method of the low voltage ride through in the doubly-fed induction generator wind turbine," in *Proc. 32nd Chin. Control Conf.*, 2013, pp. 7600–7605.
[69] S. Hu and H. Xu, "Experimental research on LVRT capability of DFIG WECS during grid voltage sags," in *Proc. Asia–Pacific Power Energy Eng. Conf.*, 2010, pp. 1–4.
[70] Y. Wang, S. Hu, D. Zhao, and H. Xu, "Low voltage ride through solution for doubly fed wind-power induction generator and experimental validation," in *Proc. Int. Conf. Electr. Mach. Syst.*, Oct. 2010, pp. 588–592.

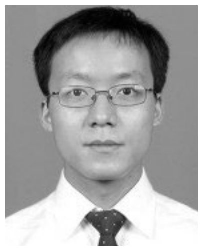

YANG HAN (Senior Member, IEEE) received the Ph.D. degree in electrical engineering from Shanghai Jiao Tong University (SJTU), Shanghai, China, in 2010.

In 2010, he joined the University of Electronic Science and Technology of China (UESTC), Chengdu, China, where he has been an Associate Professor, since 2013. From March 2014 to March 2015, he was a Visiting Scholar with the Department of Energy Technology, Aalborg University, Aalborg, Denmark. He is currently with the Department of Electrical Engineering, School of Mechanical and Electrical Engineering, UESTC. He has authored more than 20 ISI-indexed international journal articles, including three ESI highly cited articles, one ESI hot paper, and one book chapter in the areas of power electronics, power quality conditioners, and smart grid. He holds 25 issued and nine pending patents. His research interests include the ac/dc microgrids, active distribution networks, power quality, grid-connected converters for renewable energy systems, active power filters, multilevel converters, and static synchronous compensators (STATCOMs).

Dr. Han was a recipient of the Academic Talent Award by UESTC, in 2017, the Baekhyun Award by the Korean Institute of Power Electronics, in 2016, the Best Paper Awards from the 34th Annual Conference on Power System and Automation of Chinese Universities, in 2018, the Joint Conference of Sichuan Power Supply Society and Chongqing Power Supply Society, in 2018, the 6th Asia International Symposium on Mechatronics, in 2017, the 5th National Conference on Power Quality, in 2017, the Annual Conference of HVDC and Power Electronics Committee of Chinese Society of Electrical Engineers, in 2013, and the 4th International Conference on Power Quality, in 2008, China. He was a Session Chair for Power Quality and Premium Power Supply Session in 35th Annual Conference on Power System and Automation of Chinese Universities, Chengdu, China, in 2019, for Emerging Technologies and End-User Systems, Grid Operation and Management, and Power Electronics, Control and Protection Systems for Smart Grids Sessions in the IEEE PES Innovative Smart Grid Technologies Asia (ISGT Asia 2019), Chengdu, China, in 2019, for Microgrid and Distributed Generation Session in the Symposium on Power Electronics and Electrical Drives (SPEED), Xi'an, China, in 2019, for Microgrid Optimization and Scheduling Session in the 2nd International Conference on Power and Renewable Energy, Chengdu, China, in 2017, for Power Quality Mitigation and Application Session in the 5th National Conference on Power Quality, Xi'an, in 2017, and for AC/DC, DC/AC Power Converter Session in the 2016 IPEMC ECCE-Asia, Hefei, China. He is an Associate Editor for IEEE Access and the *Journal of Power Electronics* (JPE).

YU FENG received the B.S. degree in electrical engineering and automation from the University of Electronic Science and Technology of China (UESTC), Chengdu, China, in 2017, where he is currently pursuing the M.S. degree with the School of Mechanical and Electrical Engineering. His current research interests include power quality analysis, voltage sag generator, and the grid-integration of renewable energy resources.

PING YANG received the B.S. degree in mechanical engineering from Shanghai Jiao Tong University (SJTU), Shanghai, China, in 1984, and the M.S. degree in mechanical engineering from Sichuan University, in 1987.

He was visiting Victory University, Australia, from July 2004 to August 2004, and a Visiting Scholar with the S. M. Wu Manufacturing Research Center, University of Michigan, Ann Arbor, USA, from August 2009 to February 2010, and was visiting the University of California at Irvine, Irvine, USA, from October 2012 to November 2012. He is currently the Dean of the School of Mechatronics Engineering, UESTC. He is also a Full Professor with the School of Mechatronics Engineering, University of Electronic Science and Technology of China (UESTC), Chengdu, China. He has authored more than 60 articles in various journals and international conferences, and several books on mechatronics and instrumentation. His research includes mechatronics engineering, electrical engineering and automation, computer-aided control and instrumentation, smart mechatronics, and detection and automation of mechanical equipment. He received several provincial awards for his contribution in teaching and academic research.

LIN XU received the Ph.D. degree in electrical engineering from Shanghai Jiao Tong University (SJTU), Shanghai, China, in 2011. She is currently a Senior Engineering with the Sichuan Electric Power Research Institute, State Grid Sichuan Electric Power Company, Chengdu, China.

She has coauthored more than 20 journal and conference papers in the area of power electronics and power systems. Her research interests include power quality, power system analysis and real-time digital simulator (RTDS), flexible Ac transmission systems (FACTS), such as STATCOMs and power quality conditioners (DVRs, APFs). She is an Active Reviewer of the IEEE Transactions on Industrial Electronics, the IEEE Transactions on Power Electronics, and *Electric Power Components and Systems*.

YAN XU (Senior Member, IEEE) received the B.E. and M.E. degrees from the South China University of Technology, Guangzhou, China, in 2008 and 2011, respectively, and the Ph.D. degree from The University of Newcastle, Australia, in 2013. He held Postdoctoral Fellowship with The University of Sydney, Australia. He is currently an Assistant Professor with the School of Electrical and Electronic Engineering, Nanyang Technological University, Singapore. His research interests include power system stability and control, microgrid, and data-analytics for smart grid applications. He is an Editor for the IEEE Transactions on Smart Grid, the *CSEE Journal of Power and Energy Systems*, and an Associate Editor for *IET Generation, Transmission & Distribution*.

FREDE BLAABJERG (Fellow, IEEE) received the Ph.D. degree in electrical engineering from Aalborg University, in 1995. He was with ABB-Scandia, Randers, Denmark, from 1987 to 1988. He became an Assistant Professor, in 1992, an Associate Professor, in 1996, and a Full Professor of power electronics and drives, in 1998. Since 2017, he became a Villum Investigator. He has published more than 600 journal articles in the fields of power electronics and its applications. He has coauthored four monographs and an editor of ten books in power electronics and its applications. His current research interests include power electronics and its applications such as in wind turbines, PV systems, reliability, harmonics, and adjustable speed drives.

He has received the 31 IEEE Prize Paper Awards, the IEEE PELS Distinguished Service Award, in 2009, the EPE-PEMC Council Award, in 2010, the IEEE William E. Newell Power Electronics Award 2014, the Villum Kann Rasmussen Research Award 2014 and the Global Energy Prize, in 2019. He received an *honoris causa* from University Politehnica Timisoara (UPT), Romania, and Tallinn Technical University (TTU), Estonia. He was the Editor-in-Chief of the IEEE Transactions on Power Electronics, from 2006 to 2012. He has been Distinguished Lecturer for the IEEE Power Electronics Society, from 2005 to 2007, and for the IEEE Industry Applications Society, from 2010 to 2011 and 2017 to 2018. From 2019 to 2020, he serves the President for the IEEE Power Electronics Society. He is the Vice President of the Danish Academy of Technical Sciences too. He is nominated in 2014–2018 by Thomson Reuters to be between the most 250 cited researchers in Engineering in the world.